Control System Approach to the Dynamics of Nonidentical Josephson Junction Systems

Milan Stork
Dep. Applied Electronics and Telecommunications
University of West Bohemia
Plzen, Czech Republic
stork@kae.zcu.cz

Erol Kurt
Dep. Electrical and Electronics Engineering
Gazi University, Teknikokullar TR-06500,
Ankara, Turkey
ekurt52tr@yahoo.com

Abstract – **The dynamics of a resistively coupled nonidentical Josephson junction (JJ) circuit is explored and a new control strategy is applied in order to smoothen the unstable regimes. In such a system, periodic, quasiperiodic and chaotic behaviors have been encountered worldwidely. In addition, the existence of the hyperchaos has also been declared by Kurt and his coworker. It is understood that the dynamic features strictly depend on the coupling resistance R_{cp}. Indeed the decrease in R_{cp} causes a sudden increase in Lyapunov exponents, which prove the chaoticity of the system. Since a wide chaotic region is encountered, the control of the system becomes important for a number of engineering applications. A new control system approach has been applied in order to solve this problem.**

Keywords – Josephson junction, control, coupled, nonlinear, state space, system approach.

I. INTRODUCTION

Chaotic and hyperchaotic dynamics have been studied with a growing interest in the last years [1, 2] for their applications in the secure communication and synchronization [3, 4]. The chaotic systems are the ones which have one positive Lyapunov exponent with regard to its phase space dimensions [5]. If the number of the positive Lyapunov exponents increase to two, then hyperchaotic state is reached for the studied parameter. Indeed such a situation gives a rise to much complex attractors [6]. Historically, the need for chaos and hyperchaos comes from the field of secure communication. In any chaotic secure communication system, a chaotic signal is required to mask the message to be transmitted. Since the ordinary chaotic systems have one positive Lyapunov exponent, this exponent helps to mask the message. In addition, the application and practical aspects of a chaotic random number generator [7] can also be improved by different chaotic or hyperchaotic systems.

The Josephson junction (JJ) circuits attract much interest from both theoretical and experimental view, since they have some superiorities and possible technical applications over the traditional electrical circuits. The most outstanding superiorities of the superconducting circuits are their extremely small energy consumptions and pico-second range operation speeds at typical feature sizes in the micrometer range [1]. Besides, possible applications can be read as follows: The arrays of JJs exhibit important aspects in the physics and chaotic dynamics of the Josephson junctions [8]. A number of engineering applications are used with the stable rf-biased junctions, for instance, voltage standards, detectors, etc. [9]. Whereas the dc-biased junctions are used in the applications related with jamming, secure communication, synchronization and cryptography due to the co-existence of the regular and chaotic dynamics. In addition, a dc-current supply is more trustable in junctions, since an rf-supply can yield to harmonic problems [10]. On the one hand, the control of chaos becomes an active research field due to such undesirable effects which are caused by the chaoticity in the electrical or superconducting circuits [10-13]. The undesirable effects of circuits such as the Chua's circuits [14], the RL-diode circuits [12] and the periodically-excited superconducting circuits can be eliminated by using a dc-driven superconducting JJ circuit, which enables higher precision and sensitivity in time.

It is possible to control chaos both theoretically and experimentally using various ways, for instance, giving a feed-back [15], applying a weak periodic force [16-18], etc. In all of those methods, dynamic dependencies to the system parameters are vital since the desired behavior of the JJ can be determined according to this process. Thus one can operate the device either in regular region or in highly-nonlinear regimes. In this context, Nayak and Kuriakose justified a hyperchaos - chaos transition scheme in an rf-biased coupled junction [19]. One author of the present paper has proven that a dc-driven distinct and coupled Josephson circuit can generate chaos within a wider parameter region [1] compared to the study of [19].

In the present study, we explore the chaotic dynamics of a distinct coupled JJ system with regard to the parameters and focus on the control of chaos via the control system approach. It will be proven that a simpler dc-driven JJ device can generate a wide region of chaos without using an ac source compared to other studies existing in the literature. By doing so, the sensitivity of superconducting devices without the negative impacts of rf-excitation is combined with the highly-chaotic regimes in order to model a device with higher unpredictability. In addition, the control

This research has been supported by the European Regional Development Fund and the Ministry of Education, Youth and Sports of the Czech Republic under the Regional Innovation Centre for Electrical Engineering, project No. CZ.1.05/2.1.00/03.0094 and by the internal project SGS-2015-002

ISBN 978-80-261-0386-8,

scheme will be formulated and applied in order to annihilate the chaotic output from the system.

The rest of the paper is organized as follows: In Sec. 2, a brief description of the JJ system will be presented. The theory of the control scheme will be outlined in the next section. Then, Section 4 presents the dynamical results of the JJ circuits in terms of parameters and explains the results of the control scheme. Finally the concluding remarks will be discussed in the last section.

II. JUNCTION SYSTEM

A simple non-identical coupled Josephson junction (JJ) model can be drawn as in Fig. 1. One JJ system is formed by a resistively and capacitively shunted junction (RCSJ) circuit as one side of the circuit.

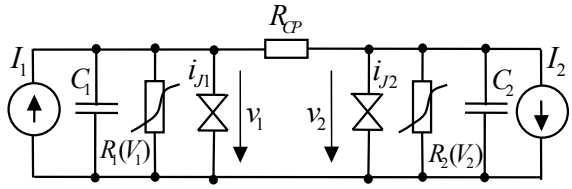

Fig. 1. The bidirectionally, resistively coupled nonidentical RC-JJ circuit

We refer to [20] for much detailed representation of this circuitry. The complete device consists of two non-identical RCSJs, which are connected to each other via a coupling resistor R_{cp}. The overall circuit can be determined with the help of Kirchoffs law as follows:

$$C_i\frac{dv_i}{dt}+\frac{v_i}{R_i(v_i)}+I_{C_i}sin\theta_i=I_i-I_{CP} \tag{1}$$

$$\frac{\hbar}{2c}\frac{d\theta_i}{dt}=v_i \tag{2}$$

$$I_{CP}=\frac{v_1+v_2}{R_{CP}} \tag{3}$$

Here, V_i is the voltage across the ith junction circuit (i = 1, 2), $\hbar = h/2\pi$ is the Planck's constant, e is the electron charge, I_i is dc current source, I_{ci} is the critical junction current, and C_i denotes the junction capacitance of the ith junction. The phase difference of the electron pairs traveling across the junction is shown by θ. For a more detailed analysis on θ, we refer to our study [21]. The phase derivatives are vital because they are proportional to the junction voltages [see Eq. (1b)]. Note that the current I_{cp} through the coupling resistance R_{cp} is given by Eq. (1c) in terms of voltage v_i on each junction. It can be seen that the coupling arises as a natural consequence of the exchange of current through the resistor R_{cp} and it depends on the total voltage on the subcircuits. In the RCSJ model [22] and [23], a nonlinear resistance $R(v)$ for each junction in Eq. (1) is defined by

$$R(v)=\begin{cases}R_n & \text{if } |v|>V_g\\ R_{SG} & \text{if } |v|\le V_g\end{cases} \tag{4}$$

Here, $V_g = 2\Delta/e$ is the gap voltage where the energy gap of JJ is denoted by Δ, and R_n and R_{sg} are nothing else than the normal state and superconducting subgap resistances, respectively. Note that the nonlinear junction resistance depends on voltage over the junction. Since we deal with the nonidentical junctions, all parameters except V_g in the nonlinear resistances are kept different for two junctions. From the numerical point of view, the dimensionless forms of the eqs. (1)-(3) should be determined in order to carry on a numerical procedure. Initially the plasma frequency,

$$\omega_j=\sqrt{\frac{2eI_{Cj}}{\hbar C_j}} \tag{5}$$

is defined for the jth RCSJ. The dimensionless form of the time is obtained by choosing one of the plasma frequencies. We chose ω_1 as

$$\tau=\omega_1 t \tag{6}$$

Then one simplifies it by replacing $V_0 = \hbar\,\omega_1/(2e)$.

$$v_j=\frac{\hbar\omega_1}{2e}\frac{d\theta_j}{d(\omega_1 t)}=V_0\frac{d\theta_j}{d\tau} \tag{7}$$

Therefore, one arrives at the dimensionless form as

$$\frac{dv_1}{dt}+g_1(v_1)v_1+sin\theta_1=\{i_1-\gamma(v_1+v_2)\} \tag{8}$$

$$\frac{d\theta_1}{d\tau}=v_1 \tag{9}$$

$$\frac{dv_2}{d\tau}+g_2(v_2)v_2+\Gamma sin\theta_2=\{i_2-\gamma(v_1+v_2)\} \tag{10}$$

$$\frac{d\theta_2}{d\tau}=v_2 \tag{11}$$

Here the parameters are defined as follows:

$$i_1=\frac{I_1}{I_{C1}},\ i_2=\frac{I_2}{I_{C2}},\ \gamma=\frac{V_0}{I_{C1}R_{CP}},\alpha=\frac{C_1}{C_2},\ \Gamma=\frac{I_{C2}C_1}{I_{C1}C_2} \tag{12}$$

$g_1(v_1)$ and $g_2(v_2)$ indicates the nonlinear resistances of the JJs:

$$g_1(v_1)=\frac{V_0}{I_{C1}R_1(v_1)}=\begin{cases}\dfrac{V_0}{I_{C1}R_1^n} & \text{if } v_1>\dfrac{V_g}{V_0}\\ \dfrac{V_0}{I_{C1}R_1^{SG}} & \text{if } v_1\le\dfrac{V_g}{V_0}\end{cases} \tag{13}$$

and

$$g_2(v_2)=\frac{C_1}{C_2}\frac{V_0}{I_{C1}R_2(v_2)}=\begin{cases}\dfrac{C_1}{C_2}\dfrac{V_0}{I_{C1}R_1^n} & \text{if } v_2>\dfrac{V_g}{V_0}\\ \dfrac{C_1}{C_2}\dfrac{V_0}{I_{C1}R_1^{SG}} & \text{if } v_2\le\dfrac{V_g}{V_0}\end{cases} \tag{14}$$

Briefly they give

$$R_1(v_1)=\begin{cases}244\,\Omega & \text{if } |v_1|>\dfrac{V_g}{V_0}\\ 0.366\,\Omega & \text{if } |v_1|\le\dfrac{V_g}{V_0}\end{cases} \tag{15}$$

$$R_2(v_2)=\begin{cases}422\,\Omega & \text{if } |v_2|>\dfrac{V_g}{V_0}\\ 0.633\,\Omega & \text{if } |v_2|\le\dfrac{V_g}{V_0}\end{cases} \tag{16}$$

where Vg = 2.26mV is considered. The resistances have been obtained from [24]. The inverse of nonlinear resistance (i.e. $1/R_i$) is the dimensionless damping factor. Besides, two critical currents are selected from [25] as $Ic1$ = 125 μA and $Ic2$ =190 μA respectively.

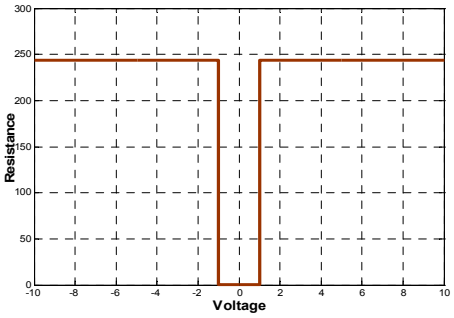

Fig. 2. Graph of nonlinear resistence R_1 versus voltage according eq. (15)

III. JUNCTION CIRCUIT AS CONTROL SYSTEM

In this part the RCSJ circuit was redraw as nonlinear electronic system with amplifier and voltage controlled current source, see Fig. 3. This electronic system is described by eq. (17).

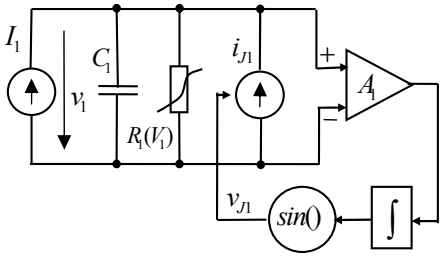

Fig. 3. The basic, single RCSJ electronic equivalen circuit diagram with amplifier, integrator and voltage controlled current source

$$\begin{aligned} C_1\frac{dv_1}{dt}+\frac{v_1}{R_1(v_1)}+i_{J1}sin\theta_1&=I_1\\ \frac{d\theta_1}{dt}&=A_1v_1\end{aligned} \tag{17}$$

The electronic versions of the resistively coupled RC-JJ are shown in Fig. 4 following Eqs. (8-11). The differential equations of electronic circuit can be converted to state space representation - as 2 control and 2 controlled systems (Fig. 5) and equations (18).

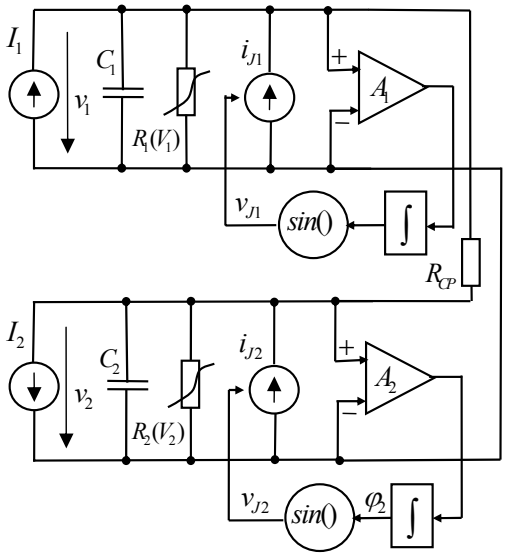

Fig. 4. The 2 bidirectionally coupled RC-JJ (equivalent cicrcuit to the Fig. 1)

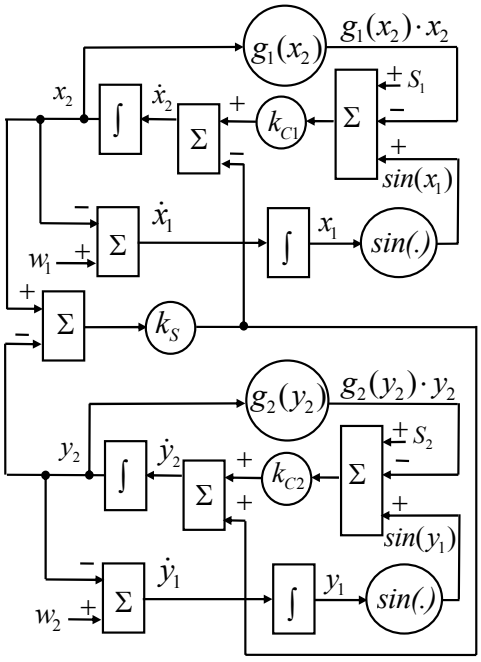

Fig. 5. The control block of the bidirectionally coupled RC-JJ (equivalent to Fig. 4)

According to Fig. 5, the integral controllers with nonlinear output function (*sin(.)*) are used in the system. In this case, one arrives at the new equations including the control procedure:

$$\begin{aligned} \frac{dx_1}{dt}&=w_1-x_2\\ \frac{dx_2}{dt}&=k_{C1}\left(S_1-g(x_2)\cdot x_2+sin(x_1)\right)-k_S\left(x_2-y_2\right)\\ \frac{dy_1}{dt}&=w_2-y_2\\ \frac{dy_2}{dt}&=k_{C2}\left(S_2-g(y_2)\cdot y_2+sin(y_1)\right)+k_S\left(x_2-y_2\right)\end{aligned} \tag{18}$$

Note that two setpoint values are w_1 and w_2 (usually = 0) and the force of systems coupling is

given by k_S. The $S_1 \equiv I_1$, $S_2 \equiv I_2$, $k_{C1} = k_{C2} = 1$ and nonlinear function $g(.)$ is

$$\begin{aligned} &if\ |x_2| \geq V_g \quad g(x_2) = 2.5\ else\ g(x_2) = 16.667 \\ &if\ |y_2| \geq V_g \quad g(y_2) = 2.5\ else\ g(y_2) = 16.667 \end{aligned} \tag{19}$$

where V_g = 0.1. The simulation results are presented in next part.

IV. Simulation Results

The systems are simulated according Eq. 18 and 19. On the beginning, the systems run separately, therefor k_S=0 is applied for time t<=400 and later k_S>0 is applied in order to perform the control scheme for t>400.

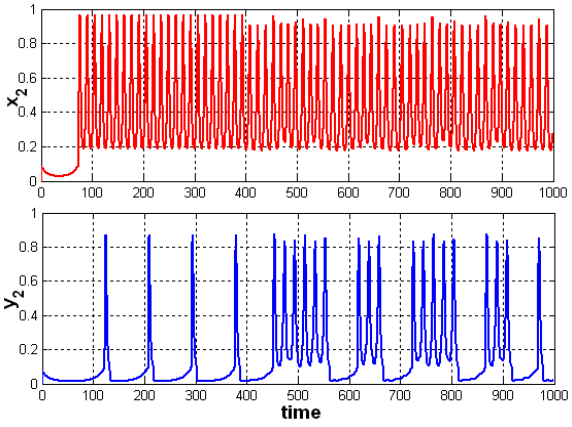

Fig. 6 Simulation results in the case of w_1=0, w_2=0. The systems are coupled for t >400; S_1=1.47; S_2=1.23; k_S=0.18

The voltage values of the first and second circuit, namely x_2 and y_2 are shown in Fig. 6. The voltage fluctuatons of two circuit are extremely different from each other. Indeed, while high frequcncy fluctuations are seen in the first circuit, the second one presents an intermittency with lower frequency. Note also that the amplitudes are similar in two circuits. The coupling parameter k_S=0.18 is too small for synchronization of the systems.

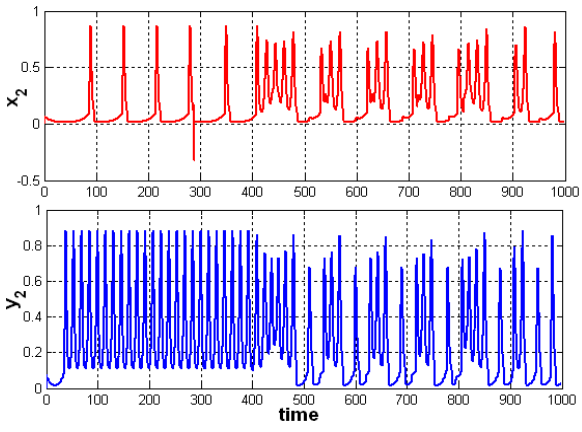

Fig. 7 Simulation w1=-0.01, w2=-0.06, systems are coupled for t>400; S_1=1.22; S_2=1.27; k_S=0.9

Fig. 7 shows the results following the coupling by using w_1=-0.01, w_2=-0.06 and k_S=0.9. Note that the coupling time for the simulation is t=400. The frequencies as well as the amplitudes fluctuate synchronously apart form the initial case shown in Fig. 6. It proves that the control of the chaotic circuit has been achieved and the synchronization of the circuits is fulfilled.

At this point, it is also interesting that the coupled Josephson junction system behaves like the bursting neurons [26]. Indeed this model can help us to understand the behavior of the neurons and implement the rules of electricity to the brain. In Fig. 8, a representative time series from the Hindmarsh-Rose (HR) model of a bursting neuron is presented [26].

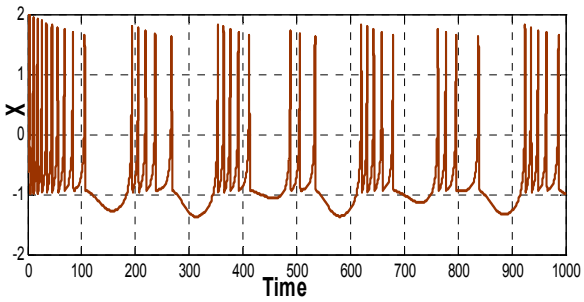

Fig. 8 Hindmarch-Rose neuron model, time diagram of state variable X for a=1, b=3, c=1, d=5, g=-1.6, ε=0.005, s=4, $I(t)$=2.9 and initial conditions: [-0.47 -2.9 2.2].

These fluctuations can be obtained from the nonlinear HR equations,

$$\left.\begin{aligned} \frac{dx}{dt} &= y - ax^3 + bx^2 - z + I(t) \\ \frac{dy}{dt} &= c - dx^2 - y \\ \frac{dz}{dt} &= \varepsilon(s(x-g) - z) \end{aligned}\right\} \tag{20}$$

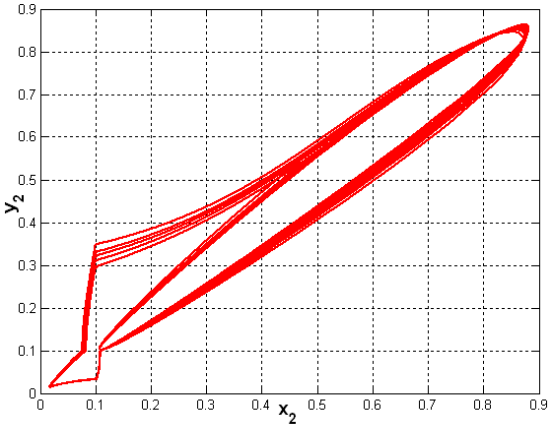

Fig. 9 Synchronization error for systems according Fig. 5, for of w_1=0, w_2=0; S_1=1.47; S_2=1.23; k_S=0.9

In Fig. 9 is shown synchronization error for systems displayed in Fig. 5. Systems are not perfectly synchronized because of phase errors and low value of k_S, but it can be corrected by means of k_S increasing, which is demonstrated in next figures.

In Fig. 10 is displayed example for the case of w_1=0, w_2=0 and S_1=1.22; S_2=1.28. The systems are coupled for t > 400 (for t<=400 k_S=0) where k_S=30. State variable x_2 is on the top, y_2 in middle and phase error = $x_2 - y_2$ bottom. In Fig. 11, the y_2 versus x_2 is shown.

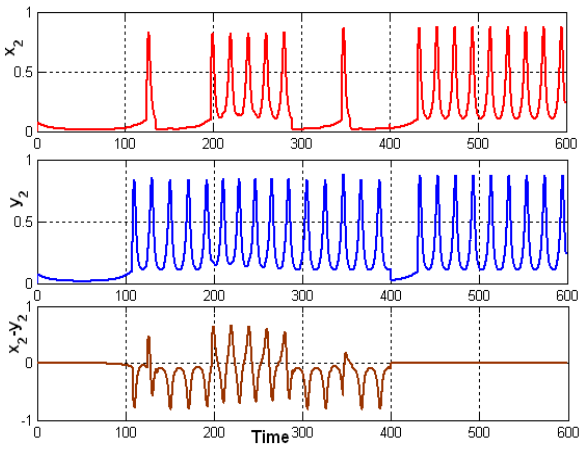

Fig. 10 Simulation results for the case of w_1=0, w_2=0. The systems are coupled for t > 400 (for t<=400 k_S=0); S_1=1.22; S_2=1.28; k_S=30. State variable x_2 is on the top, y_2 in middle and phase error = $x_2 - y_2$ bottom.

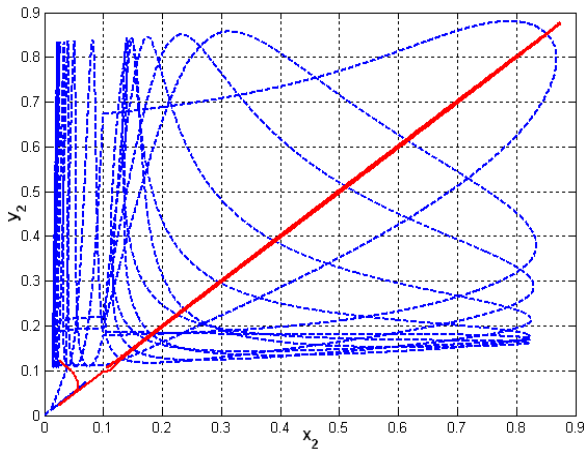

Fig. 11 Simulation results for the case of w_1=0, w_2=0. The systems are coupled for t > 400; (for t<=400 k_S=0); S_1=1.22; S_2=1.28; k_S=30. The dash line (blue) is for uncoupled systems (for t<=400 k_S=0), the solid line (red) is for coupled systems.

The results of similar example (as in Fig. 10, 11) are shown in Fig. 12 and 13, but for of w_1=0, w_2=0.11, S_1=1.22; S_2=1.29 and k_S=50. In Fig. 12 the time evolution of x2 y2 and phase error is displayed, in Fig. 13, the y_2 versus x_2 is shown.

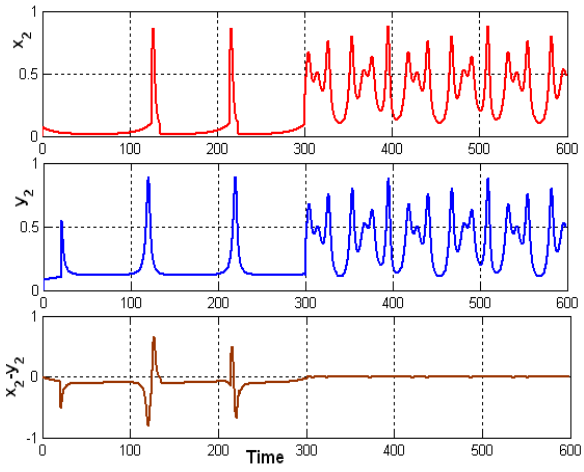

Fig. 12 Simulation results for the case of w_1=0, w_2=0.11. The systems are coupled for t > 300; S_1=1.22; S_2=1.29; k_S=50. State variable x_2 is on the top, y_2 in middle and phase error = $x_2 - y_2$ bottom.

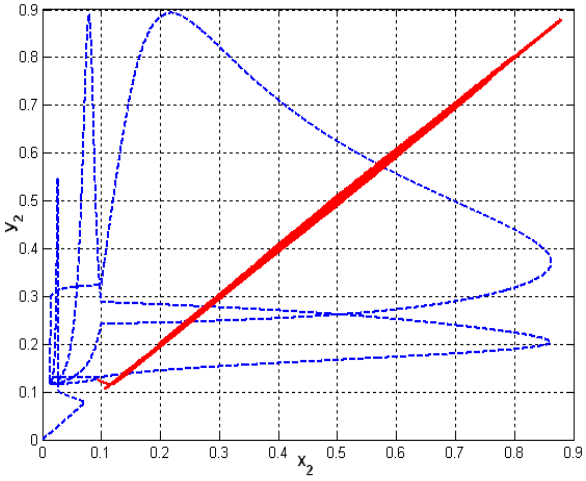

Fig. 13 Simulation results for the case of w_1=0, w_2=0.11. The systems are coupled for t > 300; (for t<=400 k_S=0); S_1=1.22; S_2=1.29; k_S=50. The dash line (blue) is for uncoupled systems (for t<=400 k_S=0), the solid line (red) is for coupled systems.

From simulation results (Fig. 10 -13) it is shown that systems are well synchronized for appropriate k_S (gain of state space variables difference $x_2 - y_2$).

V. CONCLUSION

In this paper, an electrical, nonidentical Josephson jucnction system is controlled and studied as dynamical system. Initially, the circuits fluctuate independently with different frequencies. However, after the application of control procedure, the output voltages over each junction are controlled and synchronized. It is also understood that the output signals of junctions are similar to the neuron bursts, thus electrical control model can help to understand the neuron behavior for medical purposes. Indeed synchronization studies on the neurons can be considered for future work. The control model can be technologically applied for different fields such as superconducting system, secure communication, low power fed and ultra-sensitive cryptology devices and the artificial neural applications for machine learning.

REFERENCES

[1] Kurt, E, Canturk, M, Bifurcations and hyperchaos from a dc driven non-identical Josephson junction system", *Int. J. Bifurcation and Chaos*, 20(11), pp.3725-3740, (2010).

[2] Cafagna, D., Grassi, G., New 3D-scroll attractors in hyperchaotic Chua's circuits forming a ring , *Int. J. Bifurcation and Chaos*, 13 (10), pp. 2889-2903, (2003).

[3] Udaltsov, V. S., Goedgebuer, J. P., Larger, L., Cuenot, J. B., Levy, P., Rhodes, W. T., Communicating with Hyperchaos: The Dynamics of a DNLF Emitter and Recovery of Transmitted Information, *Optics and Spectroscopy,* 95 (1), pp. 114-118, (2003).

[4] Hsieh, J. Y., Hwang, C. C., Wang, A. P., Li, W. J., Controlling hyperchaos of the Rossler system, *Int. J. Control,* 72 (10), pp. 882-886, (1999).

[5] Kurt, E., Canturk, M., Chaotic dynamics of resistively coupled DC-driven distinct Josephson junctions and the effects of circuit parameters", *Physica D: Nonlinear Phenomena*, 238(22), 2229-2237, (2009).

[6] Li, Y., Tang, W. K. S., Chen, G., Hyperchaos evolved from the generalized Lorenz equation, *Int. J. Circuit Theory Applicat.*, 33 (4), pp. 235-25, (2005).

[7] Stojanovski, T., Pihl, J., Kocarev, L., Chaos-based random number generators - Part II: Practical realization

IEEE Trans. Circuits Systems I: Fund. Theory Appl., 48 (3), pp. 382-38, (2001).

[8] Cronemeyer, D.C., Chi, C. C., Davidson, A., Pedersen, N. F., Chaos, noise, and tails on the I-V curve steps of rf-driven Josephson junctions, *Physical Review B*, 31 (5), pp. 2667-2674, (1985).

[9] Kautz, R. L., Monaco, R., Survey of chaos in the rf-biased josephson junction, *J. Appl. Physics*, 57 (3), pp. 875-889, (1985).

[10] Kapitaniak, T., *Controlling Chaos*, Academic Press, San Diego, (1996).

[11] Kurt, E., Ciylan B., Taskan, O. O., Kurt, H. H., Bifurcation analysis of a resistor-double inductor and double diode circuit and a comparison with a resistor-inductor-diode circuit in phase space and parametrical responses, *Scientia Iranica, Trans. D: Computer Sci. & Engineer. Electr. Engineer.*, 21(3), 935-944, (2014).

[12] Kasap, R., Kurt, E., Investigation of chaos in the RL-Diode circuit by using the BDS test*, J. Appl. Math. & Decision Sci.*, 2(2), (1998).

[13] Kurt, E., Acar, S., Kasap, R., A comparison of chaotic circuits from a statistical approach, *Math. & Comp. App. J.*, 2(2), (2000).

[14] E. Kurt, Nonlinearities from a non-autonomous chaotic circuit with a non-autonomous model of Chua's diode, *Physica Scripta*, 74, 22-27, (2006).

[15] Singer, J., Wang, Y.-Z., Bau, H.H., Controlling a chaotic system, *Physical Review Letters*, 66 (9), pp. 1123-1125, (1991).

[16] Balanov, A. G., Janson, N.B., Schöll, E., Delayed feedback control of chaos: Bifurcation analysis, *Physical Review E*, 71 (1), art. no. 016222, (2005).

[17] Braiman, Y., Goldhirsch, I., Taming chaotic dynamics with weak periodic perturbations, *Physical Review Letters*, 66 (20), pp. 2545-2548, (1991).

[18] Soong, C. Y., Huang, W. T., Lin, F. P., Tzeng, P. Y., Controlling chaos with weak periodic signals optimized by a genetic algorithm, *Physical Review E*, 70 (1 2), art. no. 016211, (2004).

[19] Nayak, C. R., Kuriakose, V. C., Dynamics of coupled Josephson junctions under the influence of applied fields, *Physics Letters A*, 365 (4), pp. 284-28, (2007).

[20] Barone, A., Paterno, G., *Physics and Applications of Josephson Effect*, Wiley, NY, (1982).

[21] M Canturk, E Kurt, Phase-dependent characteristics of a superconducting junction by using Schrödinger wave function, *Physica Scripta*, 76, 634-640, (2007).

[22] Dana, S. K., Sengupta, D. C., Edoh, K. D., Chaotic dynamics in Josephson Junction, *IEEE Trans. Circuits Sys.*, 48 (8), pp. 990-996, (2001).

[23] Whan, C. B., Lobb, C. J., Forrester, M. G., Effect of inductance in externally shunted Josephson tunnel junctions, *J. Applied Phys.*, 77 (1), pp. 382-389, (1995).

[24] Sarnelli, E., Testa, G., Transport properties of high-temperature grain boundary Josephson junctions *Physica C*, 371 (1), pp. 10-18, (2002).

[25] Algul, B., Avci, I., Akram, R., Bozbey, A., Tepe, M., Abukay, D., Dependence of Josephson junction critical current on the deposition rate of YBa2Cu3O7 thin films, 6. Int. Conf. Balkan Physical Union, Istanbul, Turkey, (2006).

[26] M. Stork, Bursting Oscillations of Neurons and Synchronization, 2012, 3rd International conference on Circuits, Systems, Control, Signals, WSEAS/NAUN, Barcelona, October 17-19, pp. 81-86, (2012).